communications earth & environment

ARTICLE

https://doi.org/10.1038/s43247-023-00784-8 OPEN

Ecological stability of Late Pleistocene-to-Holocene Lesotho, southern Africa, facilitated human upland habitation

Robert Patalano[1,2]✉, Charles Arthur[3], William Christopher Carleton[4,5], Sam Challis[6], Genevieve Dewar[7], Kasun Gayantha[5,8], Gerd Gleixner[8], Jana Ilgner[5], Mary Lucas[5], Sara Marzo[5,9], Rethabile Mokhachane[6,16], Kyra Pazan[10], Diana Spurite[5], Mike W. Morley[11], Adrian Parker[12], Peter Mitchell[3,6], Brian A. Stewart[6,13] & Patrick Roberts[2,5,14,15]✉

Investigation of *Homo sapiens*' palaeogeographic expansion into African mountain environments are changing the understanding of our species' adaptions to various extreme Pleistocene climates and habitats. Here, we present a vegetation and precipitation record from the Ha Makotoko rockshelter in western Lesotho, which extends from ~60,000 to 1,000 years ago. Stable carbon isotope ratios from plant wax biomarkers indicate a constant C_3-dominated ecosystem up to about 5,000 years ago, followed by C_4 grassland expansion due to increasing Holocene temperatures. Hydrogen isotope ratios indicate a drier, yet stable, Pleistocene and Early Holocene compared to a relatively wet Late Holocene. Although relatively cool and dry, the Pleistocene was ecologically reliable due to generally uniform precipitation amounts, which incentivized persistent habitation because of dependable freshwater reserves that supported rich terrestrial foods and provided prime locations for catching fish.

[1] Department of Biological and Biomedical Sciences, School of Health and Behavioral Sciences, Bryant University, Smithfield, RI, USA. [2] isoTROPIC Research Group, Max Planck Institute of Geoanthropology, Jena, Germany. [3] School of Archaeology, University of Oxford, Oxford, UK. [4] Extreme Events Research Group, Max Planck Institute for Geoanthropology, Jena, Germany. [5] Department of Archaeology, Max Planck Institute of Geoanthropology, Jena, Germany. [6] Rock Art Research Institute, University of the Witwatersrand, Johannesburg, South Africa. [7] Department of Anthropology, University of Toronto Scarborough, Toronto, ON, Canada. [8] Department of Biogeochemical Processes, Max Planck Institute for Biogeochemistry, Jena, Germany. [9] The Roslin Institute & Royal (Dick) School of Veterinary Studies, University of Edinburgh, Easter Bush Campus, Midlothian, Edinburgh, Scotland, UK. [10] Department of Anthropology, Geography, and Ethnic Studies, California State University, Stanislaus, Turlock, CA, USA. [11] College of Humanities, Arts and Social Sciences, Flinders University, Adelaide, SA, Australia. [12] School of Social Sciences, Oxford Brookes University, Headington Campus, Oxford, UK. [13] Museum of Anthropological Archaeology and Department of Anthropology, University of Michigan, Ann Arbor, MI, USA. [14] School of Social Science, The University of Queensland, Brisbane, QLD, Australia. [15] Archaeological Studies Program, University of Philippines, Diliman, Quezon City, Philippines. [16] Deceased: Rethabile Mokhachane. ✉email: rpatalan@bryant.edu; roberts@shh.mpg.de

Homo sapiens was adept at exploiting resources across varied climate zones and ecoregions within and beyond Africa by Marine Isotope Stage 3 (MIS 3, 57–29 ka)[1]. Although Late Pleistocene climatic and environmental fluctuations posed major challenges to human populations[2], people exhibited complex behavioural responses to withstand and adapt to various 'extreme' environments and associated resource instability[3–15]. Mountain systems provide an important example of this, with vulnerability to climate change, cold and dry conditions, and patchy resource distributions representing potential adaptive challenges. In the Maloti-Drakensberg Mountains of Lesotho, which divide the resource-rich southern African coast from the irregularly distributed resources of the interior (Fig. 1), *H. sapiens* appears to have inhabited cold, rugged and ecologically variable environments at altitudes greater than 1500 m above sea level (m.a.s.l.) since at least MIS 5a, or about 80 ka[10–12,14,16–19]. The Maloti-Drakensberg Mountains are a particularly key geographical feature when studying human occupation across southern Africa more generally, acting as the headwaters to the region's largest perennial rivers, the Senqu (Orange), Mohokare (Caledon), Thukela (Tugela), and Mzimvubu[20], sources of abundant and persistent freshwater for much of the surrounding region.

Southern African sites, including those of the Maloti-Drakensberg, have been argued to be crucial for understanding the early appearance of many key behavioural innovations including art, jewellery, and projectile weaponry[21–24]. However, given the historic emphasis placed on sequences from rockshelters and caves at or near the coast[25,26], it is crucial to complement this with observations from the sub-continent's topographically variable and biologically diverse interior which experienced significant climatic, environmental, and demographic changes throughout the Pleistocene[27–31]. Long-term proxy records from southern Africa show the potential impacts of changing plant landscape composition and hydroclimate on human populations over the Quaternary[32–42]. Because these environmental records are often located far from archaeological sites, however, it is important to compare these data to on-site and catchment scale (i.e., proximal) records to develop highly spatially and temporally resolved palaeoclimate and palaeoenvironmental information relevant to human evolution and behavioural change[43–46]. As a result, if we are to understand human adaptations to ecological variability associated with Late Quaternary climatic fluctuations in the interior of southern Africa, it is essential to examine records from archaeological sediments that can elucidate local responses of specific ecological communities and biomes to climatic change at sites where rich cultural assemblages have been recovered.

Lesotho forms the core of the Maloti-Drakensberg system, with two-thirds of its land area situated at elevations higher than 2000 m.a.s.l. Topographic variability and temperature variations linked to altitude and aspect produce particularly sharp gradients of warm-loving C_4 and cool-adapted C_3 plants[47–49]. Today, C_3 species flourish on the colder south-facing slopes above 2100 m.a.s.l.[12,14,18], but the transition to C_3-dominated vegetation only occurs around 2700 m.a.s.l. on warmer north-facing slopes[49–52]. As most precipitation falls during the warm summer-season, C_4 plants typically have the competitive advantage at lower altitudes. The Ha Makotoko archaeological site along the Phuthiatsana River in western Lesotho (Fig. 1C and see 'Site overview' in 'Methods'), documents pulsed occupation over the Late Pleistocene and Holocene[16,17,53]. At 10 m above the river's

Fig. 1 Location of the Ha Makotoko archaeological site in Lesotho, southern Africa. A Location of Lesotho and the boundaries of the different main rainfall zones: SRZ Summer Rainfall Zone; YRZ Year-round Rainfall Zone; WRZ Winter Rainfall Zone. **B** The location of Ha Makotoko in Lesotho in the Mesic Highveld Grassland bioregion (tan area). The Mesic Highveld Grassland is found mainly in western/northwestern Lesotho and in major river valleys while the Drakensberg Grassland (green area) is the dominant bioregion of central and eastern Lesotho[49]. **C** Location of Ha Makotoko and neighbouring Ntloana Tšoana rockshelter within the Phuthiatsana Gorge. Maps created using ArcGIS Pro desktop GIS software developed by Esri and bioregion information from ref. [49].

southern bank, Ha Makotoko was, prior to being drowned by the Metolong Dam in 2014, a large (820 m^2) rockshelter exposed to the prevailing winds of the Phuthiatsana Gorge[27], and contained evidence of a sequence of occupations starting with a Post-Howiesons Poort MSA assemblage and continuing into historic times[17,54]. Located 1640 m.a.s.l. and formed in Clarens sandstone, Ha Makotoko offers an opportunity to study past distributions of C_3 and C_4 vegetation, and to investigate the impact temperature and precipitation variability had on floral and faunal resources, as well as human behaviour, from MIS 3 to the Late Holocene.

Bulk stable carbon isotope analyses of sedimentary organic matter have documented the altitudinal movements of the C_3/C_4 vegetation gradient in response to past temperature changes from the Late Pleistocene to the Holocene in Lesotho[11,14,18]. However, the ambiguity inherent in bulk sediment isotope analysis means that it cannot reliably disentangle the source of organic matter or the influence of dominant ecological driving mechanisms on plant community composition or structure. Compound-specific isotope measurements on plant wax biomarkers, specifically normal (*n*-) alkanes, have the potential to circumvent these issues given that they provide greater specificity in terms of the origins of the organic matter being studied. Furthermore, the addition of hydrogen isotope analyses enables the assessment of past hydrological conditions of specific geographic regions. Plant wax biomarker analysis is now regularly applied in a variety of off-site[55–62] and on-site[43,63–69] sediments and soils to document human behavioural responses to changes in water availability, vegetation communities, precipitation or aridity, evapotranspiration of leaf and soil moisture, and the relative abundance of C_3 and C_4 plants. Notably, biomarker stable carbon ($\delta^{13}C$) and hydrogen (δD) isotope ratios are increasingly being used to study major processes of evolution at important hominin sites within and beyond Africa (see review[70]). Nevertheless, its application to cave and rockshelter sites linked to our species' emergence and adaptability in Africa remains limited[43,44].

Here, we present a vegetation and hydroclimate record of carbon and hydrogen isotope measurements from plant wax *n*-alkanes directly from Ha Makotoko's archaeological sediments spanning from MIS 3 to 2 (~60–26 ka), and then from the early to Late Holocene (~13–1.0 ka). Biomarker $\delta^{13}C$ and δD values from Ha Makotoko provide regional insights into the response of C_3 and C_4 plants to precipitation and temperature variability by building upon existing bulk carbon isotope data[14]. We use *n*-alkane $\delta^{13}C$ and Lesotho's well-defined altitudinal distribution of C_3 and C_4 plant taxa to estimate past temperature changes and ecological reorganizations and evaluate *n*-alkane δD as a proxy for precipitation and plant water-use efficiency. The isotopic analysis of compound-specific $\delta^{13}C$ and δD from the Ha Makotoko sedimentary sequence produces new understandings of ecological change associated with the transition from the Middle to Later Stone Age in western Lesotho and highlights the power of plant wax analyses in archaeological sediments as an exciting methodology for human evolutionary studies in southern Africa and beyond.

Results

Relative abundances of Ha Makotoko C_{29}-C_{33} and C_{31}-C_{35} *n*-alkanes are presented in Fig. 2. Plant wax biomarker distributions are dominated by odd-numbered, higher chain lengths indicating a terrestrial plant wax source (SI: Plant Wax Biomarkers). All samples have C_{31} as the dominant *n*-alkane, while the C_{29} and C_{33} homologues are the second most abundant in 4 and 12 samples, respectively. The relative contributions of C_{29} and C_{33} are moderately correlated (Spearman's correlation, $r_s = -0.807$, $p = <0.001$), co-varying in opposite directions throughout the sequence (Fig. 3). The average chain length ($ACL_{25\text{-}35}$) ranges from 29.3 to 31.2 (30.7 ± 0.5, $n = 16$), consistent with previous reports of ACL from African terrestrial plants[71,72]. The carbon preference index (CPI) of the C_{25}-C_{35} *n*-alkanes ranges between 3.0 and 11.5 (6.7 ± 2.5, $n = 16$). These values are typical of plant-derived CPI values[71,73] and indicate that no significant plant wax degradation has occurred[74].

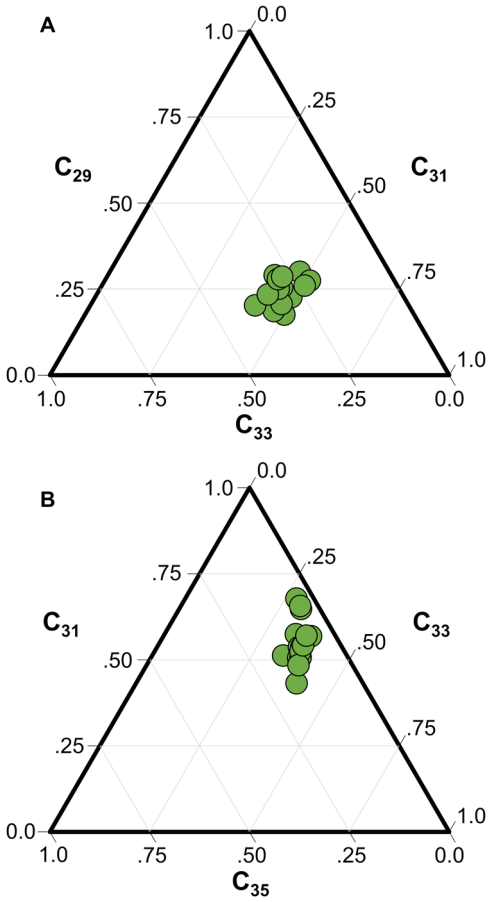

Fig. 2 Ternary diagrams for higher-chain *n*-alkane relative abundances. **A** C_{29}-C_{31} and **B** C_{31}-C_{33} *n*-alkane relative abundances. C_{31} is most dominant in all samples, typical for African vegetation.

The $\delta^{13}C$ data from the C_{29}-C_{33} *n*-alkanes show an unequivocal trend toward increasing values from the bottom to the top of Ha Makotoko's sequence (Figs. 3 and S1 and Supplementary Data 1). These range between −32.8‰ and −25.1‰ (-30.0 ± 2.1‰, $n = 45$) and, when separated by *n*-alkane homologues, between −32.8‰ and −27.6‰ (C_{29}, -30.9 ± 1.6‰, $n = 16$), −32.6‰, and −25.6‰ (C_{31}, -30.2 ± 2.4‰, $n = 15$), and −30.6‰ and −25.1‰ (C_{33}, -28.8 ± 1.7‰, $n = 14$). C_{33} *n*-alkanes displayed the highest $\delta^{13}C$ values in all but one sample (two samples did not have successful C_{33} measurements). C_{29} *n*-alkanes, on the other hand, had the lowest $\delta^{13}C$ values in all but one sample, with the largest isotopic variations between these two homologues being 3.6‰ in sediments from the Early Holocene. Although the C_{29}-C_{33} *n*-alkanes exhibit the same isotopic trends through the column, at times, there can be a ~2–3‰ difference between individual compounds, likely suggesting multiple biosynthetic sources for these three *n*-alkanes.

The δD *n*-alkane data display a general trend toward higher values from the base of the sequence to 40 cm depth (Figs. 3 and S1). In contrast to the $\delta^{13}C$ data, there is a major, mean 42.5‰, shift to lower δD values in the Late Holocene. Hydrogen isotope measurements for the C_{29}-C_{33} *n*-alkanes range between −173.3‰

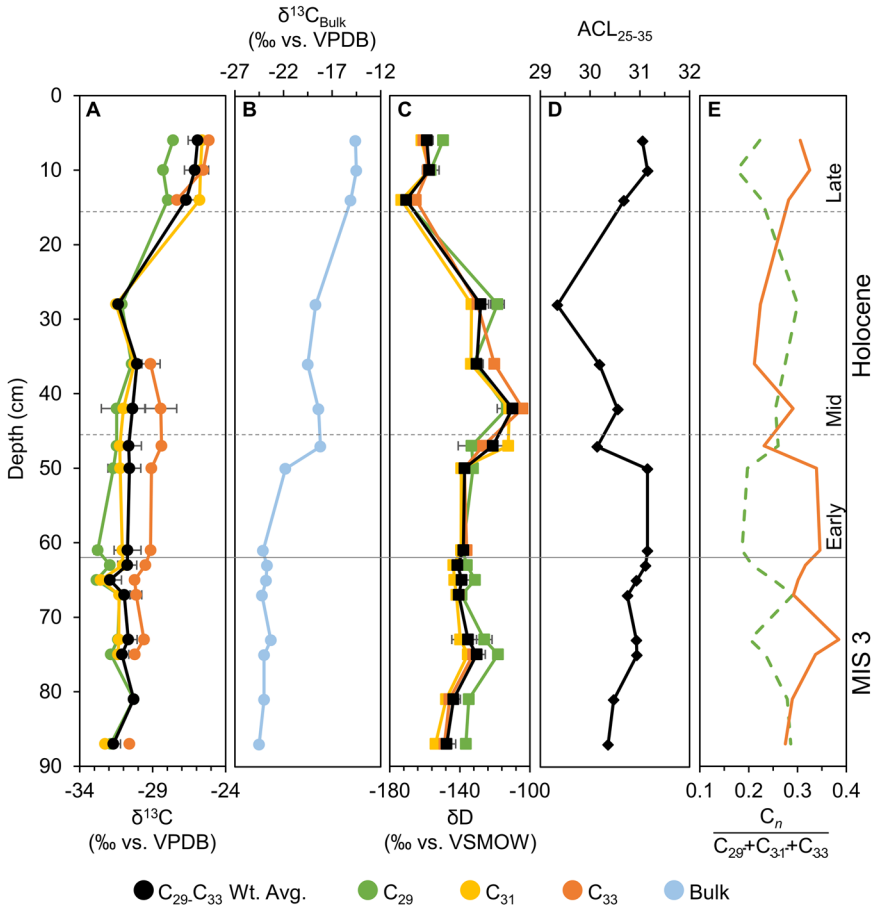

Fig. 3 Isotopic and biomarker signatures of Ha Makotoko archaeological sediments. A C_{29}-C_{33} *n*-alkane and weighted average $\delta^{13}C$ values. **B** Mean bulk $\delta^{13}C$ values for sedimentary organic matter[14]. **C** C_{29}-C_{33} *n*-alkane and weighted average δD values. **D** Average chain length (ACL) of the C_{25}-C_{35} *n*-alkanes. **E** Ratio values of C_{33} (solid, orange) and C_{29} (dashed, green) *n*-alkane abundances relative to dominant plant waxes ($C_{29} + C_{31} + C_{33}$). Higher values reflect relatively increased input of the respective compound.

and −104.3‰ (−138.4 ± 16.3‰, $n = 41$). When separated by *n*-alkane homologue, δD values range between −171.4‰ and −113.1‰ (C_{29}, −135.5 ± 14.5‰, $n = 16$), −173.3‰ and −111.8‰ (C_{31}, −141.8 ± 15.9‰, $n = 16$), and −165.1‰ and −104.3‰ (C_{33}, −139.0 ± 17.1‰, $n = 13$). The magnitudes of δD fluctuations for the C_{29}-C_{33} homologues are highly consistent and follow the same general pattern but, like $\delta^{13}C$, there can be a difference (~20‰) in δD between individual compounds, possibly suggesting differences in the source water used[75–77] or isotope variability associated with fractionation due to differences between plant ecological lifeforms[78,79].

Discussion

Effectiveness of biomarkers in archaeological contexts. As Ha Makotoko was exposed to the prevailing winds of the Phuthiatsana Gorge, aeolian plant waxes are likely to be the dominant source of rockshelter sedimentary *n*-alkanes. In terrestrial sediments, wind and dust act to ablate leaf waxes, a portion of which accumulate in the air as micrometre-sized particles[80–82]. These molecules then serve as proxy measures of the vegetation that synthesized them. We cannot rule out, however, that humans selected from specific plants surrounding the site and brought them into Ha Makotoko, or that there was a change in collecting strategies in the Late Holocene compared to older layers, which could have contributed to the observed change toward increasing C_4 input and increased precipitation. Nevertheless, climate, specifically temperature, appears to be the predominant control on vegetation distribution in Lesotho and would have influenced the availability of plants to select from or those being ablated and transported by wind (SI: Plant Type Distribution and Ecology). When other proxies from southern Africa suggest Holocene increases in temperature and precipitation (see Fig. 4 and sections below), isotope analyses and phytoliths allude to more abundant C_4 plants. This is something we also observe in our own data and, as a result, we are confident that it indicates changes in the local landscape, whether in addition to or over selection strategy changes.

Plant wax biomarkers from Ha Makotoko's sediments show excellent molecular preservation. The CPI of the C_{25}-C_{35} *n*-alkanes (Supplementary Data 1) implies that degradation is minimal, with the relatively high altitude and cool and dry setting of the rockshelter likely having helped to preserve sedimentary organic matter over time[76]. Although the wide-ranging CPI observed in modern African plants precludes its use as a single metric on which to base sample integrity[71], mature or heavily degraded samples are characterized by a considerably lower CPI of ≤1[74]. As all samples have CPI values greater than 2, the site's *n*-alkanes are well-preserved and can therefore be used to understand past climatic and environmental conditions and ecological compositions. CPI correlates weakly with $\delta^{13}C$ (Spearman's correlation, $r_s = 0.241$, $p = 0.369$) and strongly with δD (Spearman's correlation, $r_s = -0.804$, $p = <0.001$), with higher CPI values seemingly occurring during warm-wet phases and lower CPI values with cool-dry periods (Table 1 and Fig. S2).

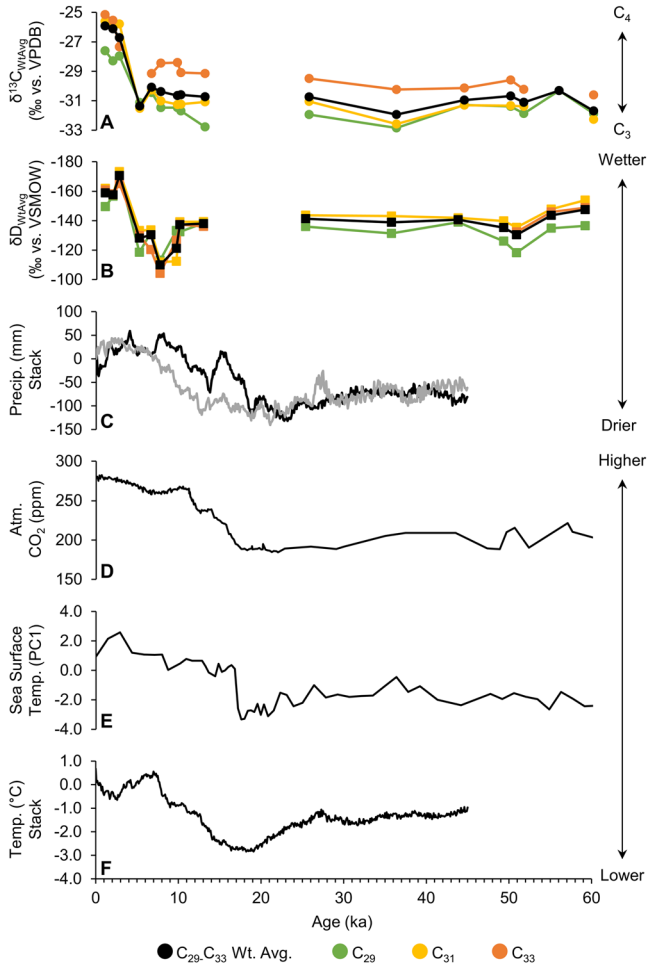

Fig. 4 Relationship between Ha Makotoko and regional climatic parameters. A C_{29}-C_{31} *n*-alkanes $\delta^{13}C$. **B** C_{29}-C_{31} *n*-alkanes δD. **C** Southern African precipitation stack of the wettest quarter for northern (grey) and central/eastern (black) SRZ[34]. **D** Global atmospheric CO_2 concentrations compiled from Dome C and Vostok ice cores, Antarctica[116–118]. **E** Principal component of SST records from MD96-2048[32]. **F** Mean annual southern African temperature stack[34].

The relative abundance of *n*-alkane biomarkers has previously been used to determine the proportional sedimentary input of C_3 woody plants and C_3 and C_4 graminoids. African woody angiosperms typically have comparatively far lower amounts of the longer chain *n*-alkanes (e.g., C_{33}, C_{35}) compared to grasses[35,71,72,83], so the relative distributions of their C_{27}-C_{35} compounds can provide context on past ecological characteristics. The dominant *n*-alkane in all 16 Ha Makotoko samples is C_{31}, with 12 samples having C_{33} as the second most prominent compound (Figs. 2 and S3). These distributions suggest that grasses were a major ecological component of the region since at least MIS 3, although woody plants also contributed waxes to the archaeological sediments, as the presence of C_{27} and C_{29} indicates[35,71,72,83,84]. Furthermore, the anti-phased relationship in the ratio values and the offset in $\delta^{13}C$ between the C_{29} and C_{33} *n*-alkanes (Fig. 3) suggests that these two biomarkers came from multiple biosynthetic sources, with their proportions possibly reflecting variability in inputs from C_3 woody plants and C_3 and C_4 graminoids[84,85]. However, we cannot exclude that vegetation brought to the site was specifically selected for by the inhabitants, as hypothesized for Diepkloof Rock Shelter, South Africa[43], and

Table 1 Spearman's r_s statistic (bottom/left) and *p* value (top/right) for all samples separated by biomarker metric and isotope values.

	n	Mean ± StDev	ACL_{25-35}	CPI_{25-35}	C_{29} $\delta^{13}C$	C_{31} $\delta^{13}C$	C_{33} $\delta^{13}C$	WtAvg $\delta^{13}C$	C_{29} δD	C_{31} δD	C_{33} δD	WtAvg δD	Bulk $\delta^{13}C$
ACL_{25-35}	16	30.7 ± 0.5	-	0.113	0.470	0.206	0.482	0.531	0.210	0.158	0.142	0.142	0.970
CPI_{25-35}	16	6.7 ± 2.5	0.412	-	0.320	0.219	0.551	0.369	0.003	<0.001	0.002	<0.001	0.676
C_{29} $\delta^{13}C^a$	16	−30.9 ± 1.6	−0.195	0.266	-	0.013	0.013	0.001	0.132	0.182	0.104	0.174	0.008
C_{31} $\delta^{13}C^a$	15	−30.2 ± 2.4	0.346	0.337	0.625	-	<0.001	<0.001	0.054	0.287	0.301	0.206	0.006
C_{33} $\delta^{13}C^a$	14	−28.8 ± 1.7	0.205	0.174	0.646	0.868	-	<0.001	0.101	0.598	0.289	0.489	<0.001
WtAvg $\delta^{13}C^a$	16	−30.0 ± 1.9	0.169	0.241	0.749	0.948	0.931	-	0.092	0.303	0.246	0.247	0.002
C_{29} δD^b	16	−135.5 ± 14.5	−0.332	−0.697	−0.393	−0.506	−0.456	−0.435	-	<0.001	<0.001	<0.001	0.629
C_{31} δD^b	16	−141.8 ± 15.9	−0.370	−0.794	−0.352	−0.294	−0.154	−0.275	0.782	-	<0.001	<0.001	0.901
C_{33} δD^b	13	−139.0 ± 17.1	−0.431	−0.780	−0.471	−0.326	−0.352	−0.347	0.863	0.978	-	<0.001	0.628
WtAvg δD^b	16	−139.4 ± 14.8	−0.384	−0.804	−0.358	−0.347	−0.202	−0.307	0.845	0.987	0.971	-	0.946
Bulk $\delta^{13}C^{a,c}$	16	−20.8 ± 3.7	0.010	0.113	0.634	0.669	0.882	0.709	−0.131	−0.034	−0.149	−0.018	-

[a]Mean reported as ‰ vs. VPDB.
[b]Mean reported as ‰ vs. VSMOW.
[c]From Roberts et al.[14].

may only represent a fraction of the plant types that comprised the local ecosystem.

Average chain length (ACL) is another metric used as a vegetation proxy because it has been shown to be higher in C_4 grasses[83], but also correlates with higher growing season temperature and aridity[85–89]. Although there was no significant difference in $ACL_{25\text{-}35}$ values between Pleistocene and Holocene samples in a Student's *t* test (two-tailed, $p = 0.506$) and Mann–Whitney *U*-test ($p = 0.958$), there are observable relationships between the $ACL_{25\text{-}35}$ and $\delta^{13}C$ and δD throughout the sequence (Fig. 3, Table 1). In general, $ACL_{25\text{-}35}$ and δD co-vary during the Pleistocene and Early through early-Mid (~13.3–6.8 ka) Holocene, with higher $ACL_{25\text{-}35}$ coinciding with higher plant wax δD. As plant wax δD values primarily record changes in precipitation amount, with less rainfall resulting in higher δD[33,90], the coincidence of higher $ACL_{25\text{-}35}$ with drier phases would suggest that longer *n*-alkanes were being produced when plants suffered from water stress in the Pleistocene[91,92]. In the later-Mid through Late Holocene (~6.8–2.0 ka), $ACL_{25\text{-}35}$ and δD are anti-phased, but $ACL_{25\text{-}35}$ and $\delta^{13}C$ co-vary and both become higher in the Late Holocene. This may indicate that a relative increase in the abundance of C_4 plants with longer chains, coinciding with elevated temperatures[85,87–89,91,93], drove $ACL_{25\text{-}35}$ and $\delta^{13}C$ values higher at this time (Figs. 3 and 4). Nevertheless, the relative abundance of *n*-alkanes from specific plant species can differ widely depending on habitat type[72,83], and chain length distributions are highly variable within plant groups, making chemotaxonomic distinctions between grasses and woody plants difficult[71].

Carbon isotope data and vegetation composition. The uncertainty associated with using plant wax distribution, CPI, and ACL as environmental indicators necessitates the application of stable isotope measurements on plant wax biomarkers to make inferences about climatic and ecosystem change. Only when the C_{29} and C_{33} distributions are compared with the measured offset between their $\delta^{13}C$ values (2.2‰ on average) can inferences be made relating to the variability of inputs from C_3 woody plants and C_3 and C_4 graminoids[84,85]. In sub-Saharan Africa, bulk and compound-specific $\delta^{13}C$ analyses have been frequently used to interpret changes in the relative past dominance of C_3 versus C_4 vegetation based on their distinct isotope ratio ranges (SI: Plant Wax Isotope Ratios). This proxy, in turn, provides insights into changes in aridity or water availability, atmospheric CO_2, temperature, and other climatic factors that influence plant community composition and structure[11,14,18,35,44,76,94–99].

The C_{29}-C_{33} weighted average of $\delta^{13}C$ values from the Pleistocene-aged Ha Makotoko samples ranges between −31.9‰ and −30.3‰ (−31.1 ± 0.6‰, $n = 7$), indicative of a C_3 ecosystem. This is comparable to previously measured bulk $\delta^{13}C$ values from this part of the Ha Makotoko sequence[14], which are also somewhat uniform, ranging from −24.5‰ to −23.3‰ (−23.9 ± 0.4‰, $n = 7$). Phytolith results from the neighbouring site of Ntloana Tšoana[53] are also dominated by C_3 grassland phytolith morphotypes during the Pleistocene, exhibiting evidence of sedges and woody vegetation (Parker et al., In prep. But also see refs. [10,18]). There is, nevertheless, some variability in the plant wax biomarkers (Table 2), as the $\delta^{13}C$ values of *n*-alkane C_{29} and C_{31} are 1–3‰ lower than those of C_{33}, with the largest difference being 2.6‰ at 65 cm depth, or ~37 ka (Fig. S1). Although all compound $\delta^{13}C$ data suggest C_3 dominance, with the low values of C_{33} that range from −30.6‰ to −29.5‰ (−30.0 ± 0.4‰, $n = 6$) being particularly diagnostic of C_3 dominating at Ha Makotoko during the Pleistocene (Figs. 3 and S1), C_{33} was likely sourced from slightly different plant ecological lifeforms (e.g., predominantly grasses) compared to C_{29} and C_{31} (e.g., grasses, trees, and shrubs)[100].

Table 2 Mann–Whitney *U*-test (bottom/left) and Kruskal–Wallis test (top/right) for *n*-alkane compound $\delta^{13}C$.

	n	Mean ± StDev[a]	C_{29}	C_{31}	C_{33}
All C_{29}	16	−30.9 ± 1.6	-	0.227	0.001
All C_{31}	15	−30.2 ± 2.4	0.235	-	0.003
All C_{33}	14	−28.8 ± 1.7	0.001	0.003	-
Pleistocene C_{29}	7	−31.6 ± 0.8	-	0.718	0.004
Pleistocene C_{31}	6	−31.7 ± 0.6	0.772	-	0.004
Pleistocene C_{33}	6	−30.0 ± 0.4	0.005	0.005	-
Holocene C_{29}	9	−30.3 ± 1.9	-	0.250	0.043
Holocene C_{31}	9	−29.3 ± 2.7	0.268	-	0.083
Holocene C_{33}	8	−27.8 ± 1.6	0.005	0.092	-

[a]Mean reported as ‰ vs. VPDB.

In the Early through Mid Holocene (~13.3–5.3 ka), *n*-alkane C_{29}-C_{33} weighted average $\delta^{13}C$ values are still low and diagnostic of C_3 plants, ranging from −31.4‰ to −30.1‰ (−30.6 ± 0.4‰, $n = 6$). There is still a large (1–4‰) discrepancy between the C_{29} and C_{31} alkanes and C_{33} $\delta^{13}C$ values during this period (Figs. 3 and 4). The bulk $\delta^{13}C$ data[14], on the other hand, suggest a shift toward a mixed C_3/C_4 ecosystem with values between −24.1‰ and −18.2‰ (−20.1 ± 2.4‰, $n = 6$) (Figs. 3 and S1). Bulk $\delta^{13}C$ values may reflect a period of acute aridity documented between ~10 and 6.8 ka (Fig. 4), as this intense dry phase correlates with a + 3.6‰ shift in bulk carbon $\delta^{13}C$[14]. Although there was an increase in the C_{33} $\delta^{13}C$ values at this time, overall, this pulse does not appear to have greatly influenced the $\delta^{13}C$ of C_{29} and C_{31} (Fig. S1), possibly due to differences in water absorption systems as outlined below. It is also possible that the bulk carbon data are recording additional sources beyond vascular plants that were not observed in the plant wax isotopes, as bulk analysis yields an average isotope ratio for the total organic component in sediments. The phytolith assemblage from the Early Holocene deposits at neighbouring Ntloana Tšoana is dominated by the presence of C_3 Pooid forms, but also includes a notable presence of Panicoids and some C_4 Chloridoids (Parker et al., In prep). Thus, the plants contributing C_{29} and C_{31} *n*-alkanes may have been better adapted to pulses of severe aridity, as a result of specific physiological adaptations related to water-use efficiency (WUE), such that they did not record a change in their $\delta^{13}C$[95]. Furthermore, trees and shrubs were likely restricted to river valleys with greater water availability. Their ability to reach water sources from deep soil horizons[79] may have helped them withstand pulses of aridity, but more modern baseline data are needed to confirm this.

Only in the Late Holocene do both bulk and compound specific $\delta^{13}C$ data show increases in the relative proportions of C_4 plants. The onset of expanding C_4 contributions to sedimentary biomarkers occurs after ~5.0 ka and is marked by a 4.6‰ increase in the weighted mean $\delta^{13}C$ and a sharp 5.7‰ increase in the C_{31} *n*-alkane at ~2.8 ka (Fig. 3). It is also in this period that C_{31} and C_{33} display similar $\delta^{13}C$ values that differ from C_{29} by 2–3‰. The bulk (−14.7 ± 0.3‰, $n = 3$) and C_{31} (−25.7 ± 0.1‰, $n = 3$) and C_{33} (−26.0 ± 1.2‰, $n = 3$) *n*-alkane $\delta^{13}C$ values all indicate an ecosystem with ample C_4 vegetation. Conversely, the corresponding −28.0‰ Late Holocene average for C_{29} is still within the C_3 isotopic range and, instead, implies a mixed C_3/C_4 ecosystem (Fig. S1). The discrepancy between the C_{29} and C_{31}-C_{33} *n*-alkanes further attests to there being multiple biosynthetic sources for the different biomarkers, complementing the evidence for variability in inputs from C_3 woody plants and both C_3 and C_4

graminoids, as reflected in their relative proportions, as well as the presence of woody taxa in the phytolith assemblage from Ntloana Tšoana. For example, the phytolith record shows an overall increased C_4 component in the Holocene, which accords with the isotope values (Parker et al., In prep.). This is also consistent with the phytolith and bulk $\delta^{13}C$ evidence of a C_4-dominated, mixed C_3/C_4 grassland at the Likoaeng archaeological site in the Senqu Valley at ~2.1 ka. Warmer conditions instigated higher frequencies of arid-adapted Chloridoid (C_4) phytoliths, lower counts of Pooid (C_3) grass phytoliths, and $\delta^{13}C$ values around −15‰[18].

Hydrogen isotope data, precipitation, and plant water-use efficiency. In southern Africa's summer rainfall zone (SRZ) (Fig. 1A), precipitation δD is determined by the amount effect, whereby increased precipitation equates to lighter δD values[33,90]. However, in mid and high latitudes, temperature variability and evapotranspiration can complicate interpretations of *n*-alkane δD (Fig. S4)[101–105]. Overall, δD values at Ha Makotoko suggest that the Pleistocene was drier relative to the Late Holocene but, for the most part, experienced consistent precipitation amounts across MIS 3, with the largest variation being about 12–17‰ between ~57 and ~53 ka (Fig. 4), coinciding with other regional records for relatively more arid climate at this time[43,44,106]. During the remainder of MIS 3, δD only varied by <5–8‰ between samples (Fig. 4B), corresponding to the relatively invariable conditions across southern Africa characterized by low but consistent precipitation amounts over MIS 3[34,106]. At Waterfall Bluff (Eastern Mpondoland, Eastern Cape Province, South Africa) and Diepkloof Rock Shelter (Western Cape Province, South Africa) relatively higher δD values suggest low rainfall conditions across MIS 3 along the coast in southern Africa's summer and winter rainfall zones[43,44].

A comparatively intense dry period marked by a high weighted average δD of −110 ± 4.8‰ is observed at Ha Makotoko ~7.9 ka, corroborating additional evidence for drier conditions in the southern African interior for this period[28,35,107–109]. Wetter conditions return after ~7.9 ka, indicated by a major 43‰ decrease in *n*-alkane δD around 2.8 ka that corresponds to high sea surface temperatures (SSTs)[32], inferred increases in southern African rainfall between 9.2 and 3.0 ka[33,34,36,110], and the intensification of summer rainfall along the eastern coast of South Africa[44]. C_4 plants also become more abundant, which could be explained by the expansion of specific C_4 taxa adapted to humid edaphic conditions. Multiple hydroclimate proxies show a positive relationship between elevated SSTs and increased precipitation in southern Africa[34] and our data, at least for the Holocene, are also indicative of this relationship.

The δD data for the C_{29}-C_{33} biomarkers are highly synchronized, suggesting that local plants had a shared water source and experienced similar environmental conditions (Fig. S1). Nevertheless, grasses, often having shorter roots, tend to use near-surface soil water deriving from recent precipitation events, whereas trees and shrubs usually have longer and deeper roots, which allow them to absorb water from deep soil horizons or groundwater aquifers[79]. δD was likely influenced by differences in plant ecological lifeform, and this could explain the ~10 to 20‰ difference between C_{29} and C_{31} and C_{33} in some samples (Table 3, Supplementary Data 1)[78,79]. Therefore, one criterion for interpreting precipitation variability through plant wax δD is to constrain vegetation changes using $\delta^{13}C$[84,111]. Sedimentary $\delta^{13}C$ and δD values throughout the sequence correlate weakly when all samples are considered together (Spearman's correlation, $r_s = -0.307$, $p = 0.247$), but isotope values are moderately correlated in the Holocene (Spearman's correlation, $r_s = -0.577$, $p = 0.110$) compared to the Pleistocene (Spearman's correlation, $r_s = -0.162$, $p = 0.733$).

Table 3 Mann–Whitney *U*-test (bottom/left) and Kruskal-Wallis test (top/right) for *n*-alkane compound δD.

	n	Mean ± StDev[a]	C_{29}	C_{31}	C_{33}
All C_{29}	16	−135.5 ± 14.5	-	0.073	0.417
All C_{31}	16	−141.8 ± 15.9	0.076	-	0.599
All C_{33}	13	−139.0 ± 17.1	0.430	0.614	-
Pleistocene C_{29}	7	−131.7 ± 7.3		0.006	0.059
Pleistocene C_{31}	7	−143.7 ± 5.9	0.007		0.850
Pleistocene C_{33}	4	−141.9 ± 7.2	0.073	0.925	
Holocene C_{29}	9	−138.4 ± 18.3		0.596	0.965
Holocene C_{31}	9	−140.3 ± 21.0	0.627		0.691
Holocene C_{33}	9	−137.7 ± 20.3	1.000	0.724	

[a]Mean reported as ‰ vs. VSMOW.

The weak linear correlation between δD and $\delta^{13}C$ values for the three biomarkers in the Pleistocene and Early Holocene implies that the overall changes in δD values were not strongly influenced by plant ecological lifeform. Conversely, plant type may exert some control on δD in the Late Holocene. Grasses, regardless of photosynthesis type, have been shown to synthesize plant waxes with lower δD[78,79,112]. Moreover, C_4 plants have greater water-use efficiency (WUE), the ratio of the rate of carbon assimilation (photosynthesis) to the rate of water loss (transpiration), than C_3 types[113]. This also results in lower *n*-alkane δD values. As the local ecology shifted from being C_3-dominant, to a mixed C_3 and C_4 grassland, a higher abundance of plants with greater WUE[33,109] supplemented the increase in southern African precipitation after ~5.0 ka[33,34,36,110], resulting in the ~40‰ decrease in plant wax δD values. The anti-phased relationship between bulk and compound-specific $\delta^{13}C$ and δD in the Late Holocene can thus be explained by prevalent C_4 plants and increased warm, summer season precipitation because, under modern CO_2 levels, the abundance of C_4 plants in a particular environment is positively correlated to high growing season temperatures and warm-season precipitation[114].

Mechanisms of ecosystem change. In contrast to most of southern Africa, where ecology is largely driven or defined by water availability[49], temperature is the most important climatic parameter in Lesotho[14,18,52]. Our $\delta^{13}C$ and δD data document this directly as the increase in C_4 plants in the Holocene positively tracks with higher temperatures and precipitation (Fig. 4). The photosynthetic efficiency of C_3 plants declines as temperatures rise, even under elevated atmospheric CO_2 concentrations[114,115]. By contrast, C_4 species outperform C_3 types as they have greater water-use efficiency and are unaffected by hot, high-light, or water-stressed conditions[95]. As most precipitation in Lesotho now falls during the southern summer (SI: Plant Wax Isotope Ratios), heightened Holocene temperatures provided a mechanism by which C_4 plants expanded in the Late Holocene at Ha Makotoko, even though CO_2 concentrations and precipitation increased[116–118], climatic factors that are both generally favourable to C_3 species. The higher $ACL_{25\text{-}35}$ values in the Late Holocene samples also help explain elevated growing season temperatures as a mechanism for ecosystem change because ACL correlates with higher growing season temperatures[85–89] and has been shown to be higher for C_4 grasses[83].

Temperature variations linked to altitude and aspect produce particularly sharp gradients of C_4 to C_3 vegetation in Lesotho, and this gradation has been used to evaluate past temperature shifts and implications for human adaptations[11,14,52]. There is roughly

a 0.6 °C change per every 100 m altitude gain/loss. Based on modern ecological studies in Lesotho, this translates to shifts in bulk grass isotopic values of approximately 2.5‰ for every 2.0 °C change[52]. The weighted average plant wax $\delta^{13}C$ from Ha Makotoko is relatively uniform across the Pleistocene (-31.1 ± 0.6‰, $n = 7$), while Holocene samples are, on average, 1.9‰ heavier (-29.2 ± 2.2‰, $n = 9$). When the Late Holocene is considered separately (-26.2 ± 0.4‰, $n = 3$), it is on average 4.8‰ and 4.4‰ higher than the Pleistocene and Early Holocene samples, respectively. Assuming shifts of 2.5‰ for every 2.0 °C change, the temperature was therefore 3.8 °C and 3.4 °C warmer in the Late Holocene compared to MIS 3 and the Early Holocene, respectively. This is consistent with the 4 °C temperature fluctuations estimated from the bulk carbon data[14].

A comparable, but smaller, 2.5 °C increase was also recorded across the Last Glacial Maximum into the Mid Holocene at Lake Mfabeni in KwaZulu-Natal, South Africa, while a larger 5 °C increase was estimated further inland at Wonderkrater, Limpopo[34,38]. Interestingly, if C_{31} is considered separately, temperature could have been nearly 5 °C warmer during the Late Holocene than MIS 3 and LGM, which is similar to estimates from multiple proxies from across southern Africa that document temperature changes as high as 6 °C during this time[14,28,29,32,34]. We must be cautious, however, as the 2.5‰ difference for every 2 °C change is estimated from bulk grass isotopes, and it is possible that bulk and compound-specific isotope analyses on soils and sediments may yield different shifts for every degree change in temperature. Modern baseline studies in this part of Lesotho are needed to further investigate the relationship between temperature and altitude change and plant wax biomarker and soil isotopes.

Implications for human occupation and resource availability. The relatively cool and dry, yet resource-reliable, Pleistocene environments along the Phuthiatsana River may have incentivized persistent habitation at Ha Makotoko and neighbouring Ntloana Tšoana[53]. Today, southern African bioregions across the sub-continent's central plateau, specifically west of the Mohokare (Caledon) River, are generally warmer but have fewer vegetation types and lower and less predictable precipitation than those in Lesotho[49]. Even with temperatures 3–5 °C cooler than today, plant wax δD values suggest drier conditions compared to the present, but generally uniform precipitation amounts across MIS 3, meaning that there would have been dependable freshwater reserves supporting rich terrestrial food resources along perennial water courses. The Phuthiatsana River itself is likely to have provided prime locations for catching fish[119], which have been argued to have underpinned the ability of hunter-gatherers to survive in upland Lesotho by compensating for significantly reduced availability of terrestrial plant foods when colder conditions prevailed[120].

The Phuthiatsana River, along with other parts of Lesotho's lowlands, and the Senqu Valley to their east, would thus have been particularly valuable to hunter-forager communities during phases of ecological instability and regional drying relative to the more uneven resource distributions of environments further inland in South Africa[11,15]. The ecological contrasts between the Maloti-Drakensberg and surrounding regions also likely played a role in the long-distance, deep time social networks that archaeologists are detecting across the region[121]. For example, the recovery of Late Pleistocene to Holocene-aged ostrich eggshell beads at the Sehonghong and Melikane rockshelters in upland Lesotho with strontium isotope values indicative of importation from interior regions >300 km away, speaks to the importance of building alliances between human societies resident in both the ecologically stable mountains and neighbouring ecological zones.

Living at the foot of the Maloti Front Range – at the interface between the mountains proper and the western interior – the inhabitants of the Phuthiatsana and adjacent foothill valleys were likely players in, and beneficiaries of, these social connections and material flows. The ability to access both the mountains and plains that lie to either side of lowland Lesotho via mobile foraging, social networking, or both, lends the Phuthiatsana an ecotonal character that would have only enhanced its long-term stability for human populations. Compound-specific biomarkers, for the first time in this region, enable us to get detailed insights into climatic and environmental variables in this critical montane heartland, as well as the ecological benefits it must have provided in a Late Pleistocene setting. With both the plant wax carbon and hydrogen isotope data providing new insights into aridity and temperature changes, this study emphasizes the importance of consistent and reliable ecological resources to persistent human occupation of Lesotho and the wider Maloti-Drakensberg region[12]. The level of potential detail available on climate-environment-human interactions from 'on-site' applications of this technique suggests that it may have wider applicability to contexts where the ecological adaptability of *Homo sapiens* and our hominin ancestors remains hotly debated[1].

Methods

Site overview and sampling. Ha Makotoko rockshelter (29°19'26"S, 27°48'13"E) was found on the south side of the Phuthiatsana River before being drowned by the Metolong Dam reservoir in 2014. It had a northwesterly aspect (300°) and received direct sunshine for much of the year, thus being on the slope face where the transition to C_3-dominated vegetation only occurs around 2700 m.a.s.l. The rockshelter had a ~60 m wide dripline, a maximum depth of 22 m, and a total area of approximately 820 m^2. Ha Makotoko was the largest rockshelter along the Phuthiatsana.

Sediment samples ($n = 21$) were taken from a geoarchaeological column adjacent to the primary excavation trench (Fig. S5) during the 2009/2010 excavations[17,53]. This, and a secondary column, were positioned at different areas of the site, specifically near the main excavation areas for the 1989 and 2009/2010 field seasons, to capture any functional changes in the internal spaces of the site. Samples were selected from the 2009/2010 column to facilitate complementary micromorphological, particle size (125 ml), phytolith (125 ml), and stable carbon isotope analyses (125 ml), including plant wax biomarkers. These were taken as loose sediment from contexts that had direct stratigraphic relationships to those in the main archaeological trench. Any sample that had visibly high concentrations of charcoal were avoided to prevent the analysis of *n*-alkanes degraded by intensive burning or heating.

There is a large sedimentation accumulation hiatus at Ha Makotoko between MIS 3 and the Holocene. Although we cannot say for certain, it is possible that changes in wind patterns either prevented rockshelter sediment accumulation or, alternatively, removed whatever had accumulated naturally. Additionally, a lack of human activity in the rockshelter may have prevented sediment buildup or worsened wind erosion of sediments. The overall occupation record of the region suggests that there may have been very few people in the area between ~30 and 13 ka, except for very brief and highly episodic visits[122]. That is, the generally colder conditions of the LGM may have instigated shifts in settlement patterns away from (certain) rockshelters, such as Ha Makotoko. Nevertheless, from the age-depth model perspective (see below), halted or eroded accumulation of sediments are equal, meaning that from the perspective of tie-points, there does not appear to be any compelling evidence of reversals or serious mixing of sediment throughout the sequence. The sedimentary structure and contexts of the geoarchaeological column and excavation trench suggests it is unlikely that the rockshelter sediments were severely turbated.

Plant biomarker extraction and isolation. Dry, homogenized sediments (~10 g, $n = 16$) were extracted with a Büchi SpeedExtractor E-916 Pressurized Speed Extractor (PSE) using 9:1 (v/v) Dichloromethane:Methanol at 100 °C and 103 bar (1500 psi) in three, 10-min cycles. Solvent containing the total lipid extract (TLE) was concentrated to ~1 mL using a Büchi SyncorePlus evaporator and then evaporated to dryness using a steady stream of N_2. The TLE was separated into Neutral, Acid, and Polar fractions by Aminopropyl column chromatography using 4 mL each of 2:1 Dichloromethane:Isopropanol, 4% Acetic Acid in Diethyl Ether, and Methanol, respectively. Normal (*n*-) alkanes were isolated from the Neutral fraction using silver nitrate infused silica gel column chromatography with 4 mL Hexane.

Molecular characterization. The *n*-alkanes were analysed with an Agilent 7890B Gas Chromatograph (GC) System equipped with an Agilent HP-5 capillary column (30 m length, 0.25 mm i.d. and 0.25 µm film), and coupled to a 5977A Series Mass Selective Detector (MSD) at the Max Planck Institute of Geoanthropology (formerly 'for the Science for Human History'), Jena, Germany. Samples were injected in pulsed split mode at 250 °C, and the GC oven was programmed from 60 °C (1 min hold) to 150 °C at 10 °C/min, then to 320 °C at 6 °C/min (10 min hold). Helium was the carrier gas with a constant flow of 1.1 mL/min. The MS source was operated at 230 °C with 70 eV ionization energy in the electron ionization (EI) mode and a full scan rate of *m/z* 50–650. Plant wax *n*-alkanes were identified by comparing mass spectra and retention times with an external C_{21}-C_{40} standard mixture.

Average chain length, or the weight-averaged number of carbon homologues of the C_{25}-C_{35} *n*-alkanes, was calculated as follows:

$$ACL = \frac{25(C_{25}) + 26(C_{26}) + \ldots + 34(C_{34}) + 35(C_{35})}{C_{25} + C_{26} + \ldots + C_{34} + C_{35}}$$

Where C_x is the abundance of the chain length with x carbons.

The carbon preference index (CPI), which examines the odd-over-even carbon number predominance and serves as an indicator for hydrocarbon maturity and degradation[74], was calculated using the abundances of odd and even chain lengths from C_{25} to C_{35} and the following formula:

$$CPI = \frac{(C_{25} + C_{27} + C_{29} + C_{31} + C_{33}) + (C_{27} + C_{29} + C_{31} + C_{33} + C_{35})}{2 \times (C_{26} + C_{28} + C_{30} + C_{32} + C_{34})}$$

There is a wide range of CPI observed in modern African plants ranging from <1 to 99, with 96.0% of all CPI values being greater than or equal to 1, 81.2% greater than or equal to 2, and 60.7% greater than or equal to 5[71]. All ACL and CPI mean values are reported with their standard deviation.

Isotope ratio characterization. Compound specific carbon isotope ratios ($\delta^{13}C$) of *n*-alkane homologues C_{25}-C_{35} were measured using an Agilent 7890A GC System equipped with an Agilent DB-1MS-UI capillary column (60 m length, 0.25 mm i.d. and 0.25 µm film), coupled to a Thermo Fisher Scientific Delta V Plus Isotope Ratio Mass Spectrometer at the Max Planck Institute for Biogeochemistry, Jena, Germany. 1.0 µL samples were injected in splitless mode at 320 °C, and the GC oven was maintained for 1 min at an initial temperature of 110 °C, before the temperature was increased to 320 °C at 5 °C/min (7 min hold). All the samples were measured in triplicates. Helium was the carrier gas with a constant flow maintained at 1.8 mL/min. We report on the C_{29}-C_{33} *n*-alkanes as they were the most abundant in all samples.

Compound specific hydrogen isotope ratios (δD) of the C_{25}-C_{35} *n*-alkanes were measured using an Agilent 7890B GC System equipped with an Agilent HP-5 MS capillary column (30 m length, 0.250 i.d. and 0.25 µm film), coupled to an Elementar Isoprime AnthrovisION Mass Spectrometer by an Elementar GC5 Furnace System Interface operated at 1050 °C at the Max Planck Institute of Geoanthropology (formerly 'for the Science for Human History'), Jena, Germany. The GC oven was temperature programmed from 60 °C (1 min hold) to 150 °C at 10 °C/min, then to 320 °C at 6 °C/min (10 min hold). Helium was the carrier gas with a constant flow of 1.1 mL/min. High purity Helium gas was introduced as three pulses into the IRMS at the start and end of each sample run to evaluate instrument performance and for standardization of the isotopic analyses. Samples were measured in triplicates. We report on the C_{29}-C_{33} *n*-alkanes as they were the most abundant in all samples.

The accuracy of the $\delta^{13}C$ and δD values were evaluated against an international standard laboratory mixture (Indiana A7, Arndt Schimmelmann, University of Indiana) injected after every three sample injections. The standard deviation of the C_{16}-C_{30} *n*-alkane working standard was ≤0.5‰ for $\delta^{13}C$ and ≤7.5‰ for δD. Drift corrections were determined by the standards run after every sample. Isotopic ratios are expressed as $\delta^{13}C$ values in per mil (‰) relative to the Vienna Pee Dee Belemnite (VPDB) standard with the following equation:

$$^{13}C = \left(\left(\frac{^{13}C}{^{12}C} Sample \div \frac{^{13}C}{^{12}C} Standard \right) - 1 \right) \times 1000$$

δD ratios are also expressed in per mil (‰) but relative to the Vienna Standard Mean Ocean Water (VSMOW) standard and the following equation:

$$\delta D = \left(\left(\frac{^{2}H}{^{1}H} Sample \div \frac{^{2}H}{^{1}H} Standard \right) - 1 \right) \times 1000$$

In addition, the H_3^+ factor was determined daily for δD measurements, having an average value of 3.06 ± 0.06, thus confirming the stability of the analytical system (the isotope software automatically corrected for H_3 contributions using the H_3^+ factor). All $\delta^{13}C$ and δD mean values are reported with their standard deviation.

Finally, Spearman's rank test was used to correlate the molecular characterizations of ACL, CPI, and the $\delta^{13}C$ and δD of the individual C_{29}-C_{33} *n*-alkanes (i.e., Table 1), while Mann–Whitney *U*-tests and Kruskal–Wallis tests were used to test the significance in differences between the C_{29}-C_{33} $\delta^{13}C$ and δD values (i.e., Tables 2 and 3). All tests were run using PAST 4.03[123] and an Alpha (α) of 0.05.

Dates and Bayesian modelling. We used the Bchronology algorithm from the R[124] package ""Bchron"[125] to create an age-depth model for Ha Makotoko. The algorithm is based on a Poisson-Gamma model for sediment accumulation. It assumes the sedimentation process is monotone (always increasing or paused, but never decreasing) and that the deposition rate can change between a given set of chronological tie-points. The tie-points consist of dated sediment layers between which the model interpolates the age-depth relationship for any desired set of depths. For the Ha Makotoko sequence, there are currently 5 radiocarbon-dated layers (Table S1) to use as tie-points. The dates were calibrated with the SHCal20 curve. For all tie-point depths we assumed a 1 cm uniform uncertainty in the depth measurements, which the Bchron model incorporates into posterior date densities.

In addition to the radiocarbon-dated layers, we used a further two tie-points. For one, we assigned a date of 0 BP (1950 AD) to the depth of 0.03 +/− 0.03 m below the surface. This date was chosen based on excavators' estimates of the age of the first few centimeters of sediment at the site. To account for uncertainty, we assumed that date was the mean of a normal distribution with a standard deviation of 30 years in line with most of the available radiocarbon dates. For the second additional tie-point, we assigned the very top of the sequence (0 m) a date of −60 BP corresponding to the start date of excavations in 2009/10. These two tie-points are effectively model priors. The rapid sedimentation implied between them in the posterior samples for the age-depth model makes the age-estimates for the uppermost 6 cm of sediment somewhat ambiguous and effectively just "modern," which accords with the excavation report. See SI Figure 6 for a plot of the model that includes upper and lower uncertainty estimates based on the 5–95% quantile ranges for interpolated ages. The plot was also produced in R with ggplot2[126]. The R code and data used to produce the age-depth model can be found on Github (https://github.com/wccarleton/hm_agedepth).

Data availability

Interpolated ages, biomarker metrices, and carbon and hydrogen isotope data have been deposited in the Figshare Database (https://doi.org/10.6084/m9.figshare.22337467). All data are also available in Supplementary Data 1. Precipitation stack of southern Africa's summer rainfall zone and mean annual southern African temperature data[34] are available from *Quaternary Science Reviews* (https://doi.org/10.1016/j.quascirev.2015.07.009). Global atmospheric CO_2 concentrations compiled from the Dome C and Vostok ice cores, Antarctica[116–118] are available in the PANGAEA database (https://doi.org/10.1594/PANGAEA.472488), *Nature* (https://doi.org/10.1038/20859), and the Environmental System Science Data Infrastructure for a Virtual Ecosystem database (https://ess-dive.lbl.gov/). Principal component of sea surface temperature records from ocean core MD96-2048[32] are found in the PANGAEA Database (https://doi.org/10.1594/PANGAEA.895366). Bulk carbon isotope data[14] are available at the *Journal of Quaternary Science* (https://doi.org/10.1002/jqs.2624).

Code availability

The R code and data used to produce the age-depth model can be found on Github (https://github.com/wccarleton/hm_agedepth).

Received: 23 September 2022; Accepted: 29 March 2023;
Published online: 20 April 2023

References

1. Roberts, P. & Stewart, B. A. Defining the 'generalist specialist' niche for Pleistocene *Homo sapiens*. *Nat. Hum. Behav.* **2**, 542–550 (2018).
2. Mackay, A., Stewart, B. A. & Chase, B. M. Coalescence and fragmentation in the late Pleistocene archaeology of southernmost Africa. *J. Hum. Evol.* **72**, 26–51 (2014).
3. Pederzani, S. et al. Subarctic climate for the earliest *Homo sapiens* in Europe. *Sci. Adv.* **7**, eabi4642 (2021).
4. Yuan, B., Huang, W. & Zhang, D. New evidence for human occupation of the northern Tibetan Plateau, China during the Late Pleistocene. *Chin. Sci. Bull.* **52**, 2675–2679 (2007).
5. Pitulko, V. V. et al. Early human presence in the Arctic: evidence from 45,000-year-old mammoth remains. *Science* **351**, 260–263 (2016).
6. Wedage, O. et al. Late Pleistocene to early-Holocene rainforest foraging in Sri Lanka: multidisciplinary analysis at Kitulgala Beli-lena. *Quat. Sci. Rev.* **231**, 106200 (2020).
7. Wedage, O. et al. Microliths in the South Asian rainforest ~45-4 ka: new insights from Fa-Hien Lena Cave, Sri Lanka. *PLoS ONE* **14**, e0222606 (2019).
8. Scerri, E. M. L. et al. Middle to Late Pleistocene human habitation in the western Nefud Desert, Saudi Arabia. *Quat. Int.* **382**, 200–214 (2015).

9. Blinkhorn, J., Achyuthan, H., Ditchfield, P. & Petraglia, M. Palaeoenvironmental dynamics and Palaeolithic occupation at Katoati, Thar Desert, India. *Quat. Res.* **87**, 298–313 (2017).
10. Stewart, B. A. et al. Afromontane foragers of the Late Pleistocene: Site formation, chronology and occupational pulsing at Melikane Rockshelter, Lesotho. *Quat. Int.* **270**, 40–60 (2012).
11. Stewart, B. A., Parker, A. G., Dewar, G., Morley, M. W. & Allott, L. F. In *Africa from MIS 6-2: Population Dynamics and Paleoenvironments* (eds Jones, S. C. & Stewart, B. A.) 247–271 (Springer Netherlands, 2016).
12. Stewart, B. A. & Mitchell, P. J. Late Quaternary palaeoclimates and human-environment dynamics of the Maloti-Drakensberg region, southern Africa. *Quat. Sci. Rev.* **196**, 1–20 (2018).
13. Loftus, E., Stewart, B. A., Dewar, G. & Lee-Thorp, J. Stable isotope evidence of late MIS 3 to middle Holocene palaeoenvironments from Sehonghong Rockshelter, eastern Lesotho. *J. Quat. Sci.* **30**, 805–816 (2015).
14. Roberts, P., Lee-Thorp, J. A., Mitchell, P. J. & Arthur, C. Stable carbon isotopic evidence for climate change across the late Pleistocene to early Holocene from Lesotho, southern Africa. *J. Quat. Sci.* **28**, 360–369 (2013).
15. Stewart, B. A. et al. Ostrich eggshell bead strontium isotopes reveal persistent macroscale social networking across late Quaternary southern Africa. *Proc. Natl Acad. Sci. USA* **117**, 6453 (2020).
16. Mitchell, P. Archaeological investigations at two Lesotho rock-shelters: the terminal Pleistocene/early Holocene assemblages from Ha Makotoko and Ntloana Tsoana. *Proc. Prehist. Soc.* **59**, 39–60 (1993).
17. Mitchell, P. & Arthur, C. Ha Makotoko: later Stone Age occupation across the Pleistocene/Holocene transition in western Lesotho. *J. Afr. Archaeol.* **12**, 205–232 (2014).
18. Parker, A. G., Lee-Thorp, J. & Mitchell, P. J. Late Holocene Neoglacial conditions from the Lesotho highlands, southern Africa: phytolith and stable carbon isotope evidence from the archaeological site of Likoaeng. *Proc. Geologists Assoc.* **122**, 201–211 (2011).
19. Pazan, K. R., Dewar, G. & Stewart, B. A. The MIS 5a (~80 ka) Middle Stone Age lithic assemblages from Melikane Rockshelter, Lesotho: highland adaptation and social fragmentation. *Quat. Int.* **611–612**, 115–133 (2022).
20. Clark, V. R., Barker, N. P. & Mucina, L. The Great Escarpment of southern Africa: a new frontier for biodiversity exploration. *Biodivers. Conserv.* **20**, 2543 (2011).
21. Mitchell, P. *The Archaeology of Southern Africa* (Cambridge University Press, 2002).
22. Robbins, L. H., Brook, G. A., Murphy, M. L., Ivester, A. H. & Campbell, A. C. In *Africa from MIS 6-2: Population Dynamics and Paleoenvironments* (eds Jones, S. C. & Stewart, B. A.) 175–193 (Springer Netherlands, 2016).
23. Dewar, G. & Stewart, B. A. In *Africa from MIS 6-2: Population Dynamics and Paleoenvironments* (eds Jones, S. C. & Stewart, B. A.) 195–212 (Springer Netherlands, 2016).
24. Wadley, L. Legacies from the Later Stone Age. *South Afr. Archaeol. Soc. Goodwin Ser.* **6**, 42–53 (1989).
25. Henshilwood, C. S. et al. An abstract drawing from the 73,000-year-old levels at Blombos Cave, South Africa. *Nature* **562**, 115–118 (2018).
26. Henshilwood, C., d'Errico, F., Vanhaeren, M., Niekerk, K. V. & Jacobs, Z. Middle Stone Age shell beads from South Africa. *Science* **304**, 404–404 (2004).
27. Arthur, C. *The Social World of Hunter-Gatherers in Early Holocene Lesotho: Integrating Method and Theory*. PhD thesis, Oxford Univ. (2018).
28. Holmgren, K. et al. Persistent millennial-scale climatic variability over the past 25,000 years in Southern Africa. *Quat. Sci. Rev.* **22**, 2311–2326 (2003).
29. Talma, A. S. & Vogel, J. C. Late Quaternary paleotemperatures derived from a speleothem from Cango Caves, Cape Province, South Africa. *Quat. Res.* **37**, 203–213 (1992).
30. Neumann, F. H., Botha, G. A. & Scott, L. 18,000 years of grassland evolution in the summer rainfall region of South Africa: evidence from Mahwaqa Mountain, KwaZulu-Natal. *Veget. Hist. Archaeobot.* **23**, 665–681 (2014).
31. Wilkins, J. et al. Innovative Homo sapiens behaviours 105,000 years ago in a wetter Kalahari. *Nature* **592**, 248–252 (2021).
32. Caley, T. et al. A two-million-year-long hydroclimatic context for hominin evolution in southeastern Africa. *Nature* **560**, 76–79 (2018).
33. Burdanowitz, N., Dupont, L., Zabel, M. & Schefuß, E. Holocene hydrologic and vegetation developments in the Orange River catchment (South Africa) and their controls. *Holocene* **28**, 1288–1300 (2018).
34. Chevalier, M. & Chase, B. M. Southeast African records reveal a coherent shift from high- to low-latitude forcing mechanisms along the east African margin across last glacial–interglacial transition. *Quater. Sci. Rev.* **125**, 117–130 (2015).
35. Kristen, I. et al. Biomarker and stable carbon isotope analyses of sedimentary organic matter from Lake Tswaing: evidence for deglacial wetness and early Holocene drought from South Africa. *J. Paleolimnol.* **44**, 143–160 (2010).
36. Zhao, X., Dupont, L., Meadows, M. E. & Wefer, G. Pollen distribution in the marine surface sediments of the mudbelt along the west coast of South Africa. *Quat. Int.* **404**, 44–56 (2016).
37. Scott, L. Vegetation history and climate in the Savanna biome South Africa since 190,000 ka: a comparison of pollen data from the Tswaing Crater (the Pretoria Saltpan) and Wonderkrater. *Quat. Int.* **57–58**, 215–223 (1999).
38. Scott, L. & Neumann, F. H. Pollen-interpreted palaeoenvironments associated with the Middle and Late Pleistocene peopling of Southern Africa. *Quat. Int.* **495**, 169–184 (2018).
39. Scott, L. & Thackeray, J. F. Mulivariate analysis of late Pleistocene and Holocene pollen spectra from Wonderkrater, Transvaal, South Africa. *South Afr. J. Sci.* **83**, 93–98 (1987).
40. Scott, L., Holmgren, K. & Partridge, T. Reconciliation of vegetation and climatic interpretations of pollen profiles and other regional records from the last 60 thousand years in the the Savanna biome of Southern Africa. *Palaeogeogr. Palaeoclimatol. Palaeocol.* **257**, 198–206 (2008).
41. Scott, L., Holmgren, K., Talma, A. S., Woodborne, S. & Vogel, J. C. Age interpretation of the Wonderkrater spring sediments and vegetation change in the Savanna Biome, Limpopo province, South Africa: research letter. *South Afr. J. Sci.* **99**, 484–488 (2003).
42. Kylander, M. E. et al. Late glacial (17,060–13,400 cal yr BP) sedimentary and paleoenvironmental evolution of the Sekhokong Range (Drakensberg), southern Africa. *PLoS ONE* **16**, e0246821 (2021).
43. Collins, J. A., Carr, A. S., Schefuß, E., Boom, A. & Sealy, J. Investigation of organic matter and biomarkers from Diepkloof Rock Shelter, South Africa: insights into Middle Stone Age site usage and palaeoclimate. *J. Archaeol. Sci.* **85**, 51–65 (2017).
44. Esteban, I. et al. Coastal palaeoenvironments and hunter-gatherer plant-use at Waterfall Bluff rock shelter in Mpondoland (South Africa) from MIS 3 to the Early Holocene. *Quat. Sci. Rev.* **250**, 106664 (2020).
45. Murungi, M. L. *Phytoliths at Sibudu (South Africa): Implications for Vegetation, Climate and Human Occupation During the MSA*. Doctor of Philosophy thesis, Univ. Witwatersrand (2017).
46. Sievers, C. Seeds from the Middle Stone Age layers at Sibudu Cave. *Southern Afr. Humanit.* **18**, 203–222 (2006).
47. Tieszen, L. L., Senyimba, M. M., Imbamba, S. K. & Troughton, J. H. The distribution of C3 and C4 grasses and carbon isotope discrimination along an altitudinal and moisture gradient in Kenya. *Oecologia* **37**, 337–350 (1979).
48. Livingstone, D. A. & Clayton, W. D. An altitudinal cline in tropical African grass floras and its paleoecological significance. *Quat. Res.* **13**, 392–402 (1980).
49. Mucina, L. & Rutherford, M. In *Strelitzia*, Vol. 19 (Sanbi, 2006).
50. Werger, M. J. A. *Biogeography and Ecology of Southern Africa*, Vol. 1 (W. Junk, 1978).
51. Vogel, J. C. Isotopic assessment of the dietary habits of ungulates. *South Afr. J. Sci.* **74**, 298–301 (1978).
52. Smith, J. M., Lee-Thorp, J. A. & Sealy, J. Stable carbon and oxygen isotopic evidence for late Pleistocene to middle Holocene climatic fluctuations in the interior of southern Africa. *J. Quat. Sci.* **17**, 683–695 (2002).
53. Mitchell, P. & Arthur, C. Archaeological fieldwork in the Metolong Dam Catchment, Lesotho, 2008–10. *Nyame Akuma* **74**, 51–62 (2010).
54. Arthur, C., Mitchell, P., Dewar, G. & Badenhorst, S. After the silt: middle and late Holocene hunter-gatherer archaeology of the Metolong Dam, Lesotho 1. *Southern Afr. Humanit.* **31**, 129–179 (2018).
55. Castañeda, I. S. et al. Wet phases in the Sahara/Sahel region and human migration patterns in North Africa. *Proc. Natl Acad. Sci. USA* **106**, 20159–20163 (2009).
56. Colcord, D. E. et al. Sub-Milankovitch paleoclimatic and paleoenvironmental variability in East Africa recorded by Pleistocene lacustrine sediments from Olduvai Gorge, Tanzania. *Palaeogeogr. Palaeoclimatol. Palaeoecol.* **495**, 284–291 (2018).
57. Feakins, S. J., deMenocal, P. B. & Eglinton, T. I. Biomarker records of late Neogene changes in northeast African vegetation. *Geology* **33**, 977–980 (2005).
58. Feakins, S. J., Eglinton, T. I. & deMenocal, P. B. A comparison of biomarker records of northeast African vegetation from lacustrine and marine sediments (ca. 3.40 Ma). *Org. Geochem.* **38**, 1607–1624 (2007).
59. Lupien, R. L. et al. A leaf wax biomarker record of early Pleistocene hydroclimate from West Turkana, Kenya. *Quat. Sci. Rev.* **186**, 225–235 (2018).
60. Lupien, R. L. et al. Abrupt climate change and its influences on hominin evolution during the early Pleistocene in the Turkana Basin, Kenya. *Quat. Sci. Rev.* **245**, 106531 (2020).
61. Lupien, R. L. et al. Vegetation change in the Baringo Basin, East Africa across the onset of Northern Hemisphere glaciation 3.3–2.6 Ma. *Palaeogeogr. Palaeoclimatol. Palaeoecol.* **570**, 109426 (2019).
62. Tierney, J. E., deMenocal, P. B. & Zander, P. D. A climatic context for the out-of-Africa migration. *Geology* **45**, 1023–1026 (2017).
63. Brittingham, A. et al. Geochemical evidence for the control of fire by Middle Palaeolithic hominins. *Nat. Sci. Rep.* **9**, 15368 (2019).
64. Connolly, R. et al. A multiproxy record of palaeoenvironmental conditions at the Middle Palaeolithic site of Abric del Pastor (Eastern Iberia). *Quat. Sci. Rev.* **225**, 106023 (2019).

65. Magill, C. R., Ashley, G. M., Domínguez-Rodrigo, M. & Freeman, K. Dietary options and behavior suggested by plant biomarker evidence in an early human habitat. *Proc. Natl Acad. Sci. USA* **113**, 2874–2879 (2015).
66. Magill, C. R., Ashley, G. M. & Freeman, K. H. Ecosystem variability and early human habitats in eastern Africa. *Proc. Natl Acad. Sci. USA* **110**, 1167–1174 (2013).
67. Magill, C. R., Ashley, G. M. & Freeman, K. H. Water, plants, and early human habitats in eastern Africa. *Proc. Natl Acad. Sci. USA* **110**, 1175–1180 (2013).
68. Patalano, R. *The Environmental Context of the Earliest Acheulean at Olduvai Gorge, Tanzania*. PhD in Archaeology thesis, Univ. Calgary (2019).
69. Uno, K. T. et al. A Pleistocene palaeovegetation record from plant wax biomarkers from the Nachukui Formation, West Turkana, Kenya. *Philos. Trans. R. Soc. B* **371**, 1–10 (2016).
70. Patalano, R., Roberts, P., Boivin, N., Petraglia, M. D. & Mercader, J. Plant wax biomarkers in human evolutionary studies. *Evol. Anthropol.* **30**, 385–398 (2021).
71. Bush, R. T. & McInerney, F. A. Leaf wax *n*-alkane distributions in and across modern plants: Implications for paleoecology and chemotaxonomy. *Geochim. Cosmochim. Acta* **117**, 161–179 (2013).
72. Vogts, A., Moossen, H., Rommerskirchen, F. & Rullkötter, J. Distribution patterns and stable carbon isotopic composition of alkanes and alkan-1-ols from plant waxes of African rain forest and savanna C_3 species. *Org. Geochem.* **40**, 1037–1054 (2009).
73. Diefendorf, A. F., Freeman, C. L., Wing, S. L. & Graham, J. M. Production of *n*-alkyl lipids in living plants and implications for the geologic past. *Geochim. Cosmochim. Acta* **75**, 7472–7485 (2011).
74. Duan, Y. & Xu, L. Distributions of *n*-alkanes and their hydrogen isotopic composition in plants from Lake Qinghai (China) and the surrounding area. *Appl. Geochem.* **27**, 806–814 (2012).
75. Bi, X., Sheng, G., Liu, X., Li, C. & Fu, J. Molecular and carbon and hydrogen isotopic composition of *n*-alkanes in plant leaf waxes. *Org. Geochem.* **36**, 1405–1417 (2005).
76. Garcin, Y. et al. Hydrogen isotope ratios of lacustrine sedimentary *n*-alkanes as proxies of tropical African hydrology: insights from a calibration transect across Cameroon. *Geochim. Cosmochim. Acta* **79**, 106–126 (2012).
77. Sachse, D. et al. Molecular paleohydrology, interpreting the hydrogen-isotopic composition of lipid biomarkers from photosynthesizing organisms. *Annu. Rev. Earth Planet. Sci.* **40**, 221–249 (2012).
78. Hou, J., D'Andrea, W. J., MacDonald, D. & Huang, Y. Evidence for water use efficiency as an important factor in determining the δD values of tree leaf waxes. *Org. Geochem.* **38**, 1251–1255 (2007).
79. Liu, W., Yang, H. & Li, L. Hydrogen isotopic compositions of *n*-alkanes from terrestrial plants correlate with their ecological life forms. *Oecologia* **150**, 330–338 (2006).
80. Rogge, W. F., Hildemann, L. M., Mazurek, M. A., Cass, G. R. & Simoneit, B. R. T. Sources of fine organic aerosol. 4. Particles shed from leaf surface of higher plants. *Environ. Sci. Technol.* **28**, 1375–1388 (1993).
81. Conte, M. H., Weber, J. C., Carlson, P. J. & Flanagan, L. B. Molecular and carbon isotopic composition of leaf wax in vegetation and aerosols in a northern prairie ecosystem. *Oecologia* **135**, 67–77 (2003).
82. Conte, M. H. & Weber, J. C. Plant biomarkers in aerosols record isotopic discrimination of terrestrial photosynthesis. *Nature* **417**, 639–641 (2002).
83. Rommerskirchen, F., Plader, A., Eglinton, G., Chikaraishi, Y. & Rullkötter, J. Chemotaxonomic significance of distribution and stable carbon isotopic composition of long-chain alkanes and alkan-1-ols in C_4 grass waxes. *Org. Geochem.* **37**, 1303–1332 (2006).
84. Wang, Y. V. et al. What does leaf wax δD from a mixed C3/C4 vegetation region tell us? *Geochim. Cosmochim. Acta* **111**, 128–139 (2013).
85. Bush, R. T. & McInerney, F. A. Influence of temperature and C_4 abundance on *n*-alkane chain length distributions across the central USA. *Org. Geochem.* **79**, 65–73 (2015).
86. Duan, Y. I. & He, J. Distribution and isotopic composition of *n*-alkanes from grass, reed and tree leaves along a latitudinal gradient in China. *Geochem. J.* **45**, 199–207 (2011).
87. Carr, A. S. et al. Leaf wax *n*-alkane distributions in arid zone South African flora: environmental controls, chemotaxonomy and palaeoecological implications. *Org. Geochem.* **67**, 72–84 (2014).
88. Castañeda, I. S., Werne, J. P., Johnson, T. C. & Filley, T. R. Late Quaternary vegetation history of southeast Africa: the molecular isotopic record from Lake Malawi. *Palaeogeogr. Palaeoclimatol. Palaeoecol.* **275**, 100–112 (2009).
89. Dodd, R. S. & Poveda, M. M. Environmental gradients and population divergence contribute to variation in cuticular wax composition in *Juniperus communis*. *Biochem. Syst. Ecol.* **31**, 1257–1270 (2003).
90. Hermann, N. et al. Hydrogen isotope fractionation of leaf wax *n*-alkanes in southern African soils. *Org. Geochem.* **109**, 1–13 (2017).
91. Sachse, D., Radke, J. & Gleixner, G. δD values of individual *n*-alkanes from terrestrial plants along a climatic gradient – Implications for the sedimentary biomarker record. *Org. Geochem.* **37**, 469–483 (2006).
92. Shepherd, T. & Wynne Griffiths, D. The effects of stress on plant cuticular waxes. *N. Phytol.* **171**, 469–499 (2006).
93. Tipple, B. J. & Pagani, M. Environmental control on eastern broadleaf forest species' leaf wax distributions and D/H ratios. *Geochim. Cosmochim. Acta* **111**, 64–77 (2013).
94. Eglinton, T. I. & Eglinton, G. Molecular proxies for paleoclimatology. *Earth Planet. Sci. Lett.* **275**, 1–16 (2008).
95. Farquhar, G. D., Hubick, K. T., Condon, A. G. & Richards, R. A. In *Stable Isotopes in Ecological Research, Vol. 68 Ecological Studies* (eds Rundel, P. W., Ehleringer, J. R. & Nagy, K. A.) Ch. 21 (Springer-Verlag, 1989).
96. O'Leary, M. Carbon isotope fractionation in plants. *Phytochemistry* **20**, 553–567 (1981).
97. Ehleringer, J. R. In *Stable Isotopes in Ecological Research*, *Vol. 68 Ecological Studies* (eds Rundel, P. W., Ehleringer, J. R. & Nagy, K. A.) Ch. 3 (Springer-Verlag, 1989).
98. Yang, H. et al. Carbon and hydrogen isotope fractionation under continuous light: implications for paleoenvironmental interpretations of the High Arctic during Paleogene warming. *Oecologia* **160**, 461–470 (2009).
99. Diefendorf, A. F., Mueller, K. E., Wing, S. L., Koch, P. L. & Freeman, K. H. Global patterns in leaf ^{13}C discrimination and implications for studies of past and future climate. *Proc. Natl Acad. Sci. USA* **107**, 5738 (2010).
100. Diefendorf, A. F. & Freimuth, E. J. Extracting the most from terrestrial plant-derived *n*-alkyl lipids and their carbon isotopes from the sedimentary record: a review. *Org. Geochem.* **103**, 1–21 (2017).
101. Kahmen, A. et al. Leaf water deuterium enrichment shapes leaf wax n-alkane δD values of angiosperm plants II: observational evidence and global implications. *Geochim. Cosmochim. Acta* **111**, 50–63 (2013).
102. Dansgaard, W. Stable isotopes in precipitation. *Tellus* **16**, 436–468 (1964).
103. Smith, F. A. & Freeman, K. H. Influence of physiology and climate on δD of leaf wax *n*-alkanes from C_3 and C_4 grasses. *Geochim. Cosmochim. Acta* **70**, 1172–1187 (2006).
104. Yapp, C. J. & Epstein, S. A re-examination of cellulose carbon bound hydrogen D measurement and some factors affecting plant–water D/H relationships. *Geochim. Cosmochim. Acta* **49**, 955–965 (1982).
105. Liu, W. & Huang, Y. Compound specific *D/H* ratios and molecular distributions of higher plant leaf waxes as novel paleoenvironmental indicators in the Chinese Loess Plateau. *Org. Geochem.* **36**, 851–860 (2005).
106. Schmidt, F., Oberhänsli, H. & Wilkes, H. Biocoenosis response to hydrological variability in Southern Africa during the last 84kaBP: a study of lipid biomarkers and compound-specific stable carbon and hydrogen isotopes from the hypersaline Lake Tswaing. *Glob. Planet. Chang.* **112**, 92–104 (2014).
107. Metwally, A. A., Scott, L., Neumann, F. H., Bamford, M. K. & Oberhänsli, H. Holocene palynology and palaeoenvironments in the Savanna Biome at Tswaing Crater, central South Africa. *Palaeogeogr. Palaeoclimatol. Palaeoecol.* **402**, 125–135 (2014).
108. Lyons, R., Tooth, S. & Duller, G. A. T. Late Quaternary climatic changes revealed by luminescence dating, mineral magnetism and diffuse reflectance spectroscopy of river terrace palaeosols: a new form of geoproxy data for the southern African interior. *Quat. Sci. Rev.* **95**, 43–59 (2014).
109. Scott, L. & Nyakale, M. Pollen indications of Holocene palaeoenvironments at Florisbad spring in the central Free State, South Africa. *Holocene* **12**, 497–503 (2002).
110. Truc, L. et al. Quantification of climate change for the last 20,000 years from Wonderkrater, South Africa: Implications for the long-term dynamics of the Intertropical Convergence Zone. *Palaeogeogr. Palaeoclimatol. Palaeoecol.* **386**, 575–587 (2013).
111. Schefuß, E., Schouten, S. & Schneider, R. R. Climatic controls on central African hydrology during the past 20,000 years. *Nature* **437**, 1003–1006 (2005).
112. Liu, W. & Yang, H. Multiple controls for the variability of hydrogen isotopic compositions in higher plant *n*-alkanes from modern ecosystems. *Glob. Chang. Biol.* **14**, 2166-2177 (2008).
113. Hatch, M. D. C_4 photosynthesis: a unique blend of modified biochemistry, anatomy and ultrastructure. *Biochem. Biophys. Acta Rev. Bioenerget.* **895**, 81–106 (1987).
114. Tipple, B. J. & Pagani, M. The early origins of terrestrial C_4 photosynthesis. *Annu. Rev. Earth Planet. Sci.* **35**, 435–461 (2007).
115. Ehleringer, J. R., Cerling, T. E. & Helliker, B. R. C_4 photosynthesis, atmospheric CO_2, and climate. *Oecologia* **112**, 285–299 (1997).
116. Monnin, E. et al. Atmospheric CO_2 concentrations over the Last Glacial Termination. *Science* **291**, 112–114 (2001).
117. Petit, J. R. et al. Climate and atmospheric history of the past 420,000 years from the Vostok ice core, Antarctica. *Nature* **399**, 429–436 (1999).
118. Pépin, L., Raynaud, D., Barnola, J. M. & Loutre, M. F. Hemispheric roles of climate forcings during glacial-interglacial transitions as deduced from the Vostok record and LLN-2D model experiments. *J. Geophys. Res. Atmos.* **106**, 31885–31892 (2001).
119. Jubb, R. A. *Freshwater Fishes of Southern Africa* (A. A. Balkema, 1967).

120. Stewart, B. A. & Mitchell, P. In *Foraging in the Past: Archaeological Studies of Hunter-Gatherer Diversity* (ed. Lemke, A.) Ch. 6 (University of Colorado Press, 2018).
121. Mitchell, P. & Stewart, B. A. In *Culturing the Body: Prehistoric Perspectives on Identity and Sociality* (eds Nowell, A. & Collins, B.) (Berghahn, in press).
122. Loftus, E., Lee-Thorp, J., Leng, M., Marean, C. & Sealy, J. Seasonal scheduling of shellfish collection in the Middle and Later Stone Ages of southern Africa. *J. Hum. Evol.* **128**, 1–16 (2019).
123. Hammer, Ø., Harper, D. A. T. & Ryan, P. D. PAST: Paleontological Statistics software package for education and data analysis. *Palaeontol. Electron.* **4**, 9 (2001).
124. R Core Team. R: a language and environment for statistical computing. https://www.R-project.org/ (2021).
125. Haslett, J. & Parnell, A. A simple monotone process with application to radiocarbon-dated depth chronologies. *J. R. Stat. Soc. Ser. C (Appl. Stat.)* **57**, 399–418 (2008).
126. Wickham, H. Ggplot2: elegant graphics for data analysis. https://ggplot2.tidyverse.org (2016).

Acknowledgements

R.P., J.I., M.L., S.M., and P.R. would like to thank the Max Planck Society for financial support. Portions of laboratory analyses were funded by the European Research Council Starter Grant PANTROPOCENE (no. 850709) awarded to P.R. C.A. and P.M. thank the Metolong Authority for its support of fieldwork at Ha Makotoko, and the World Bank, the British Academy, and the University of Oxford (through the Boise and James Fell Funds) for their financial assistance. We are grateful to Lesotho's Department of Culture and Chief Makotoko and the people of Aupolasi for permission to excavate at Ha Makotoko. A particular debt is owed to everyone who participated in the excavations. Radiocarbon dates from the site were funded by a NERC grant (2011/2/4) and we thank Dr. Tom Higham for his help in securing and interpreting them. B.A.S. gratefully acknowledges funding by the National Science Foundation, USA (Award #1724435) and the African Studies Center, University of Michigan.

Author contributions

R.P. conceptualized the study, conducted laboratory analyses and data interpretation, and wrote the manuscript. C.A. conducted fieldwork and sample collection, assisted with data interpretation, and reviewed and edited the manuscript. C.C. developed the R code to produce the age-depth model and wrote and reviewed the manuscript. S.C. conducted fieldwork and sample collection, assisted with data interpretation, and reviewed and edited the manuscript. G.D. conducted fieldwork and reviewed the manuscript. K.G. conducted laboratory analyses and data interpretation, and reviewed and edited the manuscript. G.G. assisted in data interpretation and reviewed and edited the manuscript. J.I. conducted laboratory analyses and assisted in data interpretation, and reviewed and edited the manuscript. M.L. conducted laboratory analyses and assisted in data interpretation, and reviewed and edited the manuscript. S.M. conducted laboratory analyses. R.M. conducted fieldwork and sample collection. K.P. conducted fieldwork and sample collection and reviewed and edited the manuscript. D.S. conducted laboratory analyses. M.W.M. conceptualized the study, conducted fieldwork and data interpretation, and wrote, reviewed, and edited the manuscript. A.P. conceptualized the study, conducted fieldwork and data interpretation, and wrote, reviewed, and edited the manuscript. P.M. conceptualized the study, conducted fieldwork and data interpretation, and wrote, reviewed, and edited the manuscript. B.A.S. conceptualized the study, conducted fieldwork and data interpretation, and wrote, reviewed, and edited the manuscript. P.R. conceptualized the study, conducted fieldwork and data interpretation, and wrote, reviewed, and edited the manuscript.

Funding

Open Access funding enabled and organized by Projekt DEAL.

Competing interests

The authors declare no competing interests.

Additional information

Supplementary information The online version contains supplementary material available at https://doi.org/10.1038/s43247-023-00784-8.

Correspondence and requests for materials should be addressed to Robert Patalano or Patrick Roberts.

Peer review information *Communications Earth & Environment* thanks the anonymous reviewers for their contribution to the peer review of this work. Primary handling editor: Aliénor Lavergne. Peer reviewer reports are available.

Reprints and permission information is available at http://www.nature.com/reprints

Publisher's note Springer Nature remains neutral with regard to jurisdictional claims in published maps and institutional affiliations.